Damage severity assessment of a laboratory wind turbine blade using virus optimisation algorithm

Heather Turnbull and Piotr Omenzetter

The Lloyd's Register Foundation Centre for Safety and Reliability Engineering, The University of Aberdeen

Abstract

This paper focuses on the development of a structural health monitoring (SHM) method for damage severity assessment of wind turbine blades. The methodology entails finite element model updating (FEMU) of a laboratory scale blade, accounting for uncertainty arising from measurement and modelling errors through incorporation of non-probabilistic fuzzy uncertainty quantification techniques. SHM involves continuous monitoring of the structure in operation, with dynamic responses obtained from the operational structure compared to those of the baseline with deviations in behaviour attributed to damage. In this research, the baseline model was calibrated through construction and minimisation of an objective function using a global optimisation algorithm (GOA) known as virus optimisation algorithm (VOA). Uncertainty in the blade Young's modulus and shear modulus was quantified through the fuzzy FEMU process. Then, damage severity assessment was conducted through simulating multiple damage scenarios by addition of variable masses to the structure considered to cause localised changes whilst preventing permanent structural modification. In total, four single and one concurrent scenario were considered with 50g, 100g, 200g and 400g added individually to the trailing edge, with the last scenario adding 200g to both the trailing and the leading edge. This work investigated the use of VOA for fuzzy FEMU with optimal parameters of the algorithm considered and utilised for updating. The research was able to identify all five damage scenarios simulated on the structure, with sufficient accuracy and through uncertainty quantification the potential variation associated with these parameters were unrevealed.

1   Introduction

With an increasing focus on energy generated from renewable resources, reducing associated operation and maintenance (O&M) costs would provide industry wide benefits. In relation to wind turbines, O&M costs can be prohibitively large, estimated at 20-30% of lifecycle costs for onshore turbines and 30% of the already higher lifecycle costs for offshore turbines [1]. Damage to wind turbine blades in particular can be catastrophic, with implications in terms of asset integrity, production and economic losses, and safety of personnel. Turbine blades have been identified as one of the most commonly damaged components and are crucial in the drive to reduce O&M costs. Current non-destructive methodologies involve shutdown of the turbine and travel of inspection engineers to the turbine site. As turbines are often located in remote, harsh operational environments, travel can pose risk to personnel, with bad weather caused delays to O&M scheduling. In addition, production losses occur during shutdown of the turbine and damage occurring between inspection intervals can go unnoticed.

With these limitations in mind, we propose a vibration based structural health monitoring (SHM) method based on finite element model updating (FEMU) which utilises a network of sensors permanently attached to the structure to draw conclusions about its operational health. This methodology presumes that damage accrued on the structure will manifest itself through change in the dynamic behaviour of the blade [2]. Successful application of SHM to turbine blades would provide the benefit of remote monitoring, early indication of damage to facilitate maintenance scheduling as appropriate, as well as monitoring of the structure after extreme unpredictable events such as lightning strikes.

FEMU is an inverse technique using responses of the blade to calibrate unknown parameters enabling a prediction to be made about the operational state of the structure. Responses of the

blade are measured in its baseline state, with the responses of the operational blade monitored continuously and any significant deviations directly attributed to damage. In its basic form, FEMU is a deterministic process, giving no consideration to uncertainty arising from sources such as uncertain test data or numerical model idealisations and therefore is considered idealistic when considering real world engineering problems. Uncertainty quantification (UQ) methods known as probabilistic and non-probabilistic quantification have been developed to account for various uncertainties. Probabilistic methods, based on well-known probability theory assigns unknown variables with probability density functions (PDFs), however the form of these PDFs are rarely known a priori and are based upon assumptions and engineering judgment. Non-probabilistic UQ, such as fuzzy methods adopted in this research model uncertainty in the output parameters as membership functions and propagate this uncertainty through the FEM to obtain an estimate of uncertain input parameters. As a result, they make no initial assumptions regarding the distribution of input parameters.

Probabilistic UQ applied to FEMU of bridges was carried out by Hua et al. [3] and Behmanesh and Moaveni [4], while Chandrashekhar and Ganguli [5] and Simoen et al. [6] applied the methodology to damage detection of an RC beam. Due to the aforementioned limitations associated with probabilistic methods, non-probabilistic methods such as interval and those based on fuzzy logic were adopted in this research. To account for epistemic uncertainties in model updating, Erdogan and Bakir [7] proposed a general FFEMU framework in which responses were modelled as fuzzy numbers to account for measurement error, with this used to understand uncertainty associated with structural parameters. This work demonstrated FFEMU in the context of damage detection of a reinforced frame structure. Liu and Duan [8] applied FFEMU accounting for measurement error through fuzzification of the objective function. They were able to obtain multiple potential models, with varying degrees of fuzziness and select the most physically compatible using engineering judgment. In dealing with aleatory uncertainty, Khodaparast et al. [9] built fuzzy membership functions of responses through histograms obtained from repeated assembly and disassembly of the DLR AIRMOD structure. The authors built these membership functions and used a kriging predictor meta-model to construct fuzzy input variables.

This research will apply the non-probabilistic UQ method known as fuzzy finite element model updating (FFEMU) to account for measurement and modelling uncertainties in the updating process. The research will conduct damage severity assessment of a wind turbine blade subject to imitated operational conditions through non-destructively simulating multiple damage scenarios upon the structure. Damage will be simulated through addition of masses of varying magnitudes to the structure to cause alterations. The FFEMU optimisation problem will be solved using virus optimisation algorithm (VOA) for minimisation of the fuzzy objective functions, providing a novelty aspect of this research.

2 Methodology

The FEMU process involves calibrating a numerical model based on the results obtained from an experimental campaign, to create a numerical model which better reflects the true dynamics of the system. This section will demonstrate the methodology adopted in this research for these components with section 2.1.1 introducing the experimental configuration and modal analysis procedure undertaken. The numerical model created will be discussed in section 2.1.2, which will be updated using the FFEMU process. This involves the construction and minimisation of both deterministic and fuzzy objective functions as defined in section 2.1.3. To facilitate minimisation of these objective functions the GOA described in section 2.1.4 will be utilised. To facilitate damage severity assessment studies, damage will be simulated both experimentally on the test specimen and numerically on the FEM, a description of both methodologies can be found in section 2.1.5. A discussion surrounding the physical implementation of the algorithm can be found in section 2.1.6.
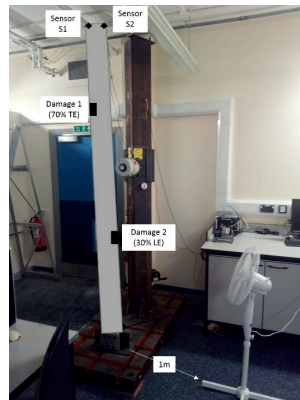
Figure 1 - Experimental configuration with excitation source (fan), and sensor and damage locations

2.1.1 Experimental configuration

A 2.36 m blade from a Fortis domestic scale wind turbine with 5 kW power output and 5 m rotor diameter was situated in a laboratory environment. The blade material was presumed to be glass-fibre reinforced epoxy composite although detailed material specifications were unavailable from the manufacturer. The blade has an E387 aerofoil cross-section which is continuous through its length. Mass and mass density of the blade, obtained from measurements were 7.11 kg and 2,300 kg/m^3, respectively. The blade was oriented in a vertical fixed-free configuration, to represent the parked position of a blade, and clamped to a heavy steel base. To simulate an un-measurable wind-like excitation, a pedestal fan with 0.41 m rotor diameter was located at a distance of approx. 1 m from the blade leading edge (LE) as shown in Figure 1. Operational modal analysis (OMA) was utilised to extract the modal parameters of the blade. OMA was used to extract only frequency values, therefore, it was sufficient to capture the response using one miniature piezo electric accelerometer model Metra KS94B-100 with a weight of 3.2 g, voltage sensitivity of 98.95 mV/g and operational frequency range of 0.5-28 kHz. Acceleration readings were taken with a sampling rate of 2,048 Hz with a measurement time of 30 minutes. The collected acceleration signals were digitised with a National Instruments NI-9234 data acquisition card connected to a NI cDAQ-9174 chassis and laptop. NI LabView software was used for signal processing. To extract the modal parameters from the collected acceleration responses, a system identification algorithm known as frequency domain decomposition (FDD) was used. Detailed information about FDD can be found in [11].

2.1.2 Numerical model

The numerical model of the blade was created using ABAQUS software. The blade was modelled as a beam with generalised cross section to reduce complexity of modelling. The cross-sectional values used for the generalised cross section were estimated using a shape builder software as shown in Table 1. The blade was modelled using 140 B31 beam elements, with the centre of mass and centre of stiffness offset to capture the eccentricity of the E387 profile. The clamped experimental boundary condition was reproduced through an encastre boundary condition imposed upon the bottom node of the blade model. An initial estimate of material properties was obtained from Soden et al. [12] assuming the blade to be an epoxy composite material with unidirectional glass fibre reinforcement known as E-glass 21xK43 Gevetex. Initially, the Young's modulus was assumed to be 53.48 GPa while shear modulus was assumed as 5.83 GPa, respectively. These parameters were used as an initial estimate and to build the feasibility regions of potential solutions, however, as they were updated during the baseline phase, their accuracy was not of concern.

2.1.3 Fuzzy finite element model updating

FEMU involves calibration of an FEM using responses obtained from an experimental campaign, allowing the FEM to be reflective of the true dynamics of the system. FEMU using global optimisation algorithms (GOAs) involves creating an objective function containing modal parameters from both the analytical model and experimental specimen and minimising the discrepancy between the two to obtain a set of updated input parameters. The introduction of fuzzy theory, developed by Zadeh [13], allows responses to be modelled as fuzzy numbers with the sub-level technique used to assign each level a membership function value. In this regard, a membership function value $\mu=1$ indicates that the object is surely a member of the set, while a membership function value $\mu=0$ indicates the member does not belong to the set. A membership function value between these extremities indicates the value belongs to the set with a given degree of membership. In this research, we model responses as triangular membership functions, with sub-levels $\mu=1$, $\mu=0.75$, $\mu=0.5$, $\mu=0.25$, $\mu=0$.

2.1.3.1 Objective functions

Two types of objective functions are required for FFEMU, one which is deterministic and another which is fuzzy in nature. The desired output of the deterministic objective function is an updated vector of input parameters that minimises the discrepancy between deterministic experimental and analytical modal parameters. Considering only frequency values during updating, this objective function can be written as:

$$f(\boldsymbol{\theta}) = \sum_{i=1}^{n} \left[\frac{\lambda_i^a(\boldsymbol{\theta}) - \lambda_i^e}{\lambda_i^e} \right]^2 \tag{1}$$

where λ_i represents the ith natural frequency value, a and e refer to the analytical and experimental frequencies and n is the number of frequencies considered during updating. This function is only applicable to updating level $\mu=1$. For the remaining fuzzy sub-levels, fuzzy objective functions must be formulated which provides interval updating parameter vectors that minimise modal parameter discrepancy at the bounds. The fuzzy objective functions are specified as $\underline{f}(\boldsymbol{\theta}^I)$ and $\overline{f}(\boldsymbol{\theta}^I)$ for the lower and upper bounds, respectively. The fuzzy objective functions adopted in this research are as follows:

$$\underline{f}(\boldsymbol{\theta}^I) = \underline{\mathbf{r}}^T(\boldsymbol{\theta}^I)\mathbf{W}\underline{\mathbf{r}}(\boldsymbol{\theta}^I) \tag{2}$$

$$\overline{f}(\boldsymbol{\theta}^I) = \overline{\mathbf{r}}^T(\boldsymbol{\theta}^I)\mathbf{W}\overline{\mathbf{r}}(\boldsymbol{\theta}^I) \tag{3}$$

where $\boldsymbol{\theta}^I$ is the interval updating parameter vector, and $\mathbf{W}$ is the weighting matrix. The residuals at the lower and upper bounds are denoted as $\underline{\mathbf{r}}$ and $\overline{\mathbf{r}}$, respectively, and calculated as

$$\underline{\mathbf{r}}_i(\boldsymbol{\theta}^I) = \left(\underline{\lambda}_i^a(\boldsymbol{\theta}^I) - \underline{\lambda}_i^e\right)\Big/\underline{\lambda}_i^e \qquad \overline{\mathbf{r}}_i(\boldsymbol{\theta}^I) = \left(\overline{\lambda}_i^a(\boldsymbol{\theta}^I) - \overline{\lambda}_i^e\right)\Big/\overline{\lambda}_i^e \tag{4}$$

2.1.4 Virus optimisation algorithm

Virus optimisation algorithm (VOA), originally developed by Liang et al. [14], is a metaheuristic optimisation algorithm, inspired by the spread of virus through a host cell. The algorithm draws on multiple bio-analogies. The algorithm can be divided into three main phases:

- Initialisation

- Replication
- Anti-virus/immunity response

During the initialisation phase, viruses (potential solutions) are randomly generated within the feasibility region with their ability to spread determined dependant on their calculated objective function value. Viruses with a low objective function value will be considered as "strong" and allowed to replicate at a higher rate than those with a higher objective function value and "common" attribute. The higher replication rate will promote exploitation of promising regions, while replication of common viruses will promote exploration of the wider solution space.

During the replication phase, new strong viruses, $\mathbf{SV}_{ij}^{n}$, are created according to the following formula:

$$\mathbf{SV}_{ij}^{n} = \mathbf{SV}_{ij} \pm \frac{rand}{intensity} \times \mathbf{SV}_{ij} \qquad (5)$$

where $\mathbf{SV}_{ij}$ is the parameter vector associated with the strong virus, $rand$ is a randomly generated number, and $intensity$ controls the random perturbation of new viruses created from the original ones. When the algorithm has not found a better solution after replication, exploration is intensified through increasing the $intensity$ value. Subscripts i and j represents the jth dimension of the ith particle in the population. The main purpose of common viruses is exploration of the cell, searching the wider solution domain for better solutions. They replicate at a lesser rate, with new solutions generated according to:

$$\mathbf{CV}_{ij}^{n} = \mathbf{CV}_{ij} \pm rand \times \mathbf{CV}_{ij} \qquad (6)$$

After replication of viruses, the anti-virus mechanism is triggered to provide some protection to the host cell by elimination of a random number of viruses from the population at each iteration. As the number of viruses killed at each iteration is variable, the population size is dynamic. Additionally, to maintain manageability of the population once the user-defined population threshold value is reached the number of viruses is reduced to its originally specified size. In this study, we took the minimum number of strong members in the population at any given time to be twenty.

2.1.5 Damage simulation

As opposed to destructively damaging the experimental specimen, mass was added to the structure to simulate a structural alteration. Typical damage locations of operational wind turbines were investigated by Ciang et al. and Ataya and Ahmed [15, 16], concluding that damage commonly occurred at 30% length and 70% length on the blade LE and TE, respectively. The mass magnitude and locations used in each damage scenario can be seen in Table 2. This technique for non-destructive experimental damage simulation has been used previously by e.g. Behmanesh and Moaveni [4]. To simulate damage analytically, the baseline FEM described in section 2.1.2 with updated material properties was adapted to include two potential damage locations as shown in Figure 2. The potential locations were chosen based on assumed knowledge of the experimentally simulated damage scenarios. As a result, parameters M_7 and M_{13} were modelled as non-structural masses with variable magnitudes and considered as updating parameters during the optimisation process.

2.1.6 Algorithm implementation

The algorithm was coded in MATLAB software with the modal properties of the analytical blade obtained using ABAQUS2MATLAB toolbox developed by Papazafeiropoulos et al. [17]. To increase computational efficiency, the University of Aberdeen's high-performance

computing cluster was used, with parallel computing ability exploited through parallelisation of the code at each iteration.

<div style="display: flex;">
<div>

Table 1 – Cross-sectional properties of E387 aerofoil profile

Variable	Value
Area (m^2)	1.29 x10^{-3}
Moment inertia for bending about x-axis (m^4)	1.54x10^{-8}
Mixed moment of inertia for (m^4)	2.40x10^{-9}
Moment inertia for bending about y-axis (m^4)	1.42x10^{-6}
Torsional constant (m^4)	5.28x10^{-8}
Centre of mass (m)	(0.00, 0.00)
Centre of stiffness (m)	(-7.05x10^{-3}, 1.96x10^{-3})

</div>
<div>

Table 2 – Experimental damage scenario mass magnitudes

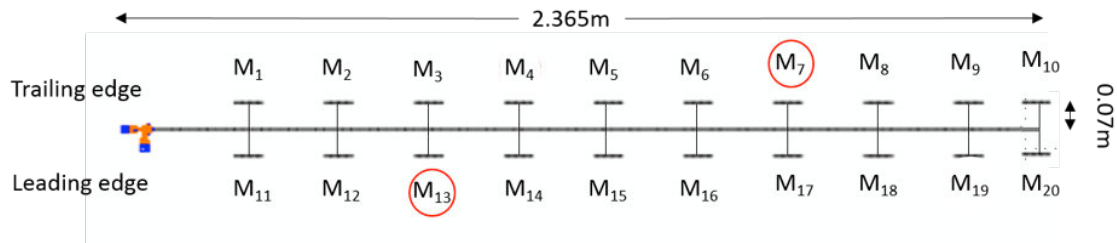| Scenario	Mass (g)	Distance f/base (% length)	Updating parameter	Edge
1	50	70	M_7	TE
2	100	70	M_7	TE
3	200	70	M_7	TE
4	400	70	M_7	TE
5	200 & 200	70 & 30	M_7 & M_{13}	TE & LE

</div>
</div>

Figure 2 - Numerical damage model in ABAQUS with damage locations

3   Results

The dynamic properties of the blade, obtained through experimental modal analysis procedures are detailed in section 3.1.1. The properties obtained for baseline and each of the damage states will be utilised in sections 3.1.2-3.1.4 for calibration of the baseline model and subsequent damage prediction studies. Section 3.1.2 will act as a parameter setting exercise, examining individually the modifiable parameters of VOA to achieve the optimum configuration of the algorithm. Section 3.1.3 will discuss the application of VOA to baseline updating, with section 3.1.1.2 using these results for damage prediction.

3.1.1   Experimental results

3.1.1.1 Baseline model

The experimental campaign undertaken on the blade without modification provided the first ten natural frequency values shown in Table 3. The results detailed here are an average value achieved over five runs of OMA, with close values achieved for each mode in all five runs.

3.1.1.2 Damage scenarios

To simulate experimental structural modification, the mass magnitudes detailed in Table 2 were added to the blade in the locations specified. The first ten natural frequency values obtained for each damage scenario can be seen in Table 4. The structural modification scenarios implemented in this research are sufficient to discern between the naturally occurring variability and that due directly to damage simulation. The mass magnitudes selected have a varying affect upon the deviation in modal properties, causing a relative frequency variation between practically 0% and 12.3%.

Table 3 - Experimental natural frequencies of blade in baseline state using FDD

Mode number	Bending/Torsional	Average frequency (Hz)
1	B	1.75
2	B	11.2
3	B	31.3
4	T	38.9
5	B	61.3
6	B	100.2
7	T	116.8
8	B	149.3
9	T	194.7
10	B	207.2

Table 4 - Experimental natural frequencies of blade in damage states using FDD with percentage variation wrt. baseline state

Mode No.	Damage Scenario 1		Damage Scenario 2		Damage Scenario 3		Damage Scenario 4		Damage Scenario 5	
	Frequency (Hz)	Relative difference (%)	Frequency (Hz)	Relative difference (%)	Frequency (Hz)	Relative difference (%)	Frequency (Hz)	Relative difference (%)	Frequency (Hz)	Relative difference (%)
1	1.75	-0.1	1.73	-0.9	1.72	-1.5	1.69	-3.5	1.72	-1.7
2	11.2	0.0	11.2	-0.2	11.2	-0.4	11.1	-0.9	11.0	-1.9
3	31.2	-0.5	30.9	-1.3	30.6	-2.2	29.7	-5.5	29.7	-5.3
4	38.0	-2.2	37.1	-4.7	37.1	-5.0	35.7	-8.8	37.0	-5.1
5	61.2	-0.2	61.0	-0.5	60.9	-0.7	60.6	-1.2	60.3	-1.7
6	100.1	-0.1	100.2	0.0	100.1	-0.1	100.0	-0.2	100.0	-0.2
7	116.7	-0.1	116.6	-0.2	116.2	-0.5	116.3	-0.4	112.5	-3.9
8	148.1	-0.8	149.0	-0.2	145.5	-2.6	141.5	-5.5	142.8	-4.6
9	190.7	-2.0	191.6	-1.6	186.2	-4.6	173.4	-12.3	184.0	-5.8
10	205.8	-0.7	205.4	-0.9	203.9	-1.6	201.7	-2.7	199.6	-3.8

3.1.2 VOA optimal parameter investigation

Setting suitable parameters for VOA is crucial for successful implementation of the algorithm. Suitable parameters were investigated for deterministic updating of the baseline state before proceeding with damage state updating. The main user specified parametric variables in VOA are initial number of solutions, growth rate of strong and common viruses and the algorithm anti-virus threshold. Using knowledge obtained from a previous own study [10] in relation to the perceived global minimum objective function value achieved by particle swarm optimisation (PSO) and firefly algorithm (FA), variables were altered individually with their ability to achieve the known minimum compared. The parametric investigation consisted of seven cases (Table 5), each run three times with the results averaged due to the randomness associated with initial solution generations. The parameters that remained constant throughout this investigation were those recommended by Liang et al. [14]. The size of the initial population specified was seen to influence the ability to reach a good solution, with 25 and 50 viruses found to be unsuitable in all cases. In addition to this, adjusting the growth rate of strong and common viruses was found to influence the algorithms success rate, with case 5 providing a good compromise between exploration and exploitation of the solution space. The anti-virus mechanism was generally found to be beneficial while increasing the population reduction threshold enabled the algorithm to achieve good solutions at each run, it, however, required significantly more evaluations. The optimum configuration of this algorithm was judged to be:
- Initial population –100

- Growth rate of common viruses – 6
- Growth rate of strong viruses – 10
- Anti-virus mechanism - on
- Population reduction threshold – 2000.

The optimum parameter configuration detailed above was able to achieve convergence on the same minimum solution, with slightly higher objective function value compared to the deterministic updating using PSO and FA shown in Table 6 [10]. To visualise the VOA through various iterations, a snapshot of the population of viruses was taken at selected iterations, as shown in Figure 3. At the first iteration, the randomly populated viruses are evenly distributed throughout the solution domain. As the algorithm moves onto its second iteration, the number of viruses is seen to grow with the most significant growth observed for strong solutions. By the third iteration, viruses appear to be focusing on exploitation of the region near the minimum value, however, with the threshold of strong viruses set to be any objective function value below 0.001, exploration of the wider solution domain is continued in the future iterations. By the tenth iteration, the population, consisting only of strong viruses, has found the minimum value and has searched the region in its vicinity for a better solution.

3.1.3 Baseline model updating

Deterministic updating of the baseline model was carried out using the optimal parameter configuration detailed in section 3.1.2. The baseline model was updated well, with the relative error in frequencies obtained between initial model and VOA updated model seen to decrease from 19.2% to 1.7% as shown in Table 7. Uncertainty was introduced into the numerical results following the methodology defined by Simoen et al. [6]. For fuzzy updating of the baseline model, to understand the uncertainty associated with material properties, the sublevels were updated individually to obtain an updating parameter vector at both lower and upper bounds of the level. These updating parameter vectors were then assembled to give the results shown in Figure 4.

Table 5 - Updating baseline deterministic model with various VOA parameter settings

	Case number						
	1	2	3	4	5	6	7
Number of initial solutions	**25**	**50**	**100**	100	100	100	100
Growth rate - common viruses	4	4	4	**3**	**6**	4	4
Growth rate - strong viruses	7	7	7	**5**	**10**	7	7
Anti-virus (on/off)	on	on	on	on	on	**off**	on
Population reduction threshold	1000	1000	1000	1000	1000	1000	**2000**
Minimum objective value	7.81×10^{-5}	2.14×10^{-5}	8.47×10^{-7}	3.70×10^{-6}	2.27×10^{-7}	8.58×10^{-7}	2.27×10^{-7}
No. of function evaluations	11268	6345	3964	7799	6905	6484	11585

Table 6 - Updating parameters and objective function values achieved by PSO, FA and VOA with optimal parameters

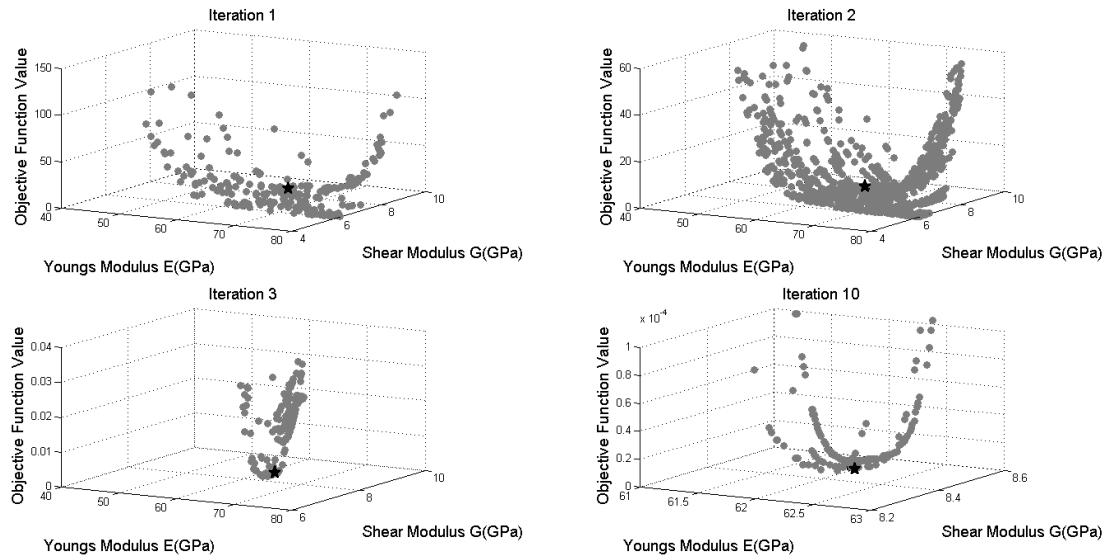| Algorithm	E (GPa)	G (GPa)	Objective function value
PSO	61.9	8.5	2.08×10^{-7}
FA	61.9	8.5	2.08×10^{-7}
VOA	61.9	8.5	2.14×10^{-7}

Figure 3 -VOA iterations showing population of viruses at iterations 1, 2, 3 and 10 (grey dots = viruses, black star = minimum value of objective function)

Table 7 - Comparison between experimental, initial model and VOA updated models for deterministic baseline updating

Frequency no.	1	2	3	4	5	6	7	8	9	10
Experimental (Hz)	1.75	11.2	31.3	38.9	61.3	100.6	116.6	149.2	194.6	207.2
Initial model (Hz)	1.65	10.4	29.0	32.1	56.7	92.9	139.0	160.2	193.3	224.2
Initial error (%)	-5. 5	-7.6	-7.6	-17.5	-7.6	-7.7	19.2	7.4	-0.7	8.2
VOA (Hz)	1.8	11.2	31.2	38.7	61.0	100.6	116.7	149.9	193.1	208.8
Updated error (%)	1.7	-0.6	-0.5	-0.5	-0.5	0.0	0.1	0.5	-0.7	0.8
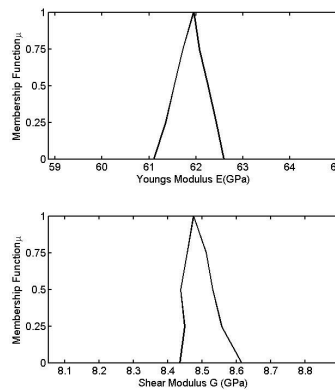
Figure 4 - Fuzzy updated material parameters obtained using VOA

3.1.4 Damage model updating

Deterministic updating was undertaken utilising the experimental results obtained from various alteration scenarios detailed in section 3.1.1.2. Deterministic results were considered individually, with the experimentally simulated damage predicted well for each of the five scenarios as seen in Figure 5. The accuracy demonstrated was sufficient for the four individual damage scenarios, whilst the concurrent scenario (scenario 5) showed an under prediction of M_7 and over prediction of M_{13}. Results obtained from deterministic damage updating in previous

own studies using FA [10] have been shown for comparison. As the methodology would be used for damage prediction, this knowledge would trigger an inspection therefore perfect accuracy of the method may not be required.

After deterministic updating, uncertainty was introduced to each of the results in Table 4 and propagated back through the FEM using the FFEMU procedure to understand the uncertainty associated with the updating parameters. The fuzzy updated mass parameters obtained from each damage scenario are visualised in Figure 6 with a comparison to the experimental mass shown by the dashed line. In each case, the experimental mass magnitude lies within the range of uncertainty, with each case indicating damage is surely present in the correct region. In all singular damage scenarios (1-4), a small magnitude of mass was predicted analytically on location M_{13} where it had not been simulated experimentally. This result was consistent through all scenarios but considerably smaller than the magnitude of mass predicted on the location of actual experimental mass M_7. When considering the case of concurrent damage, the membership functions of parameter M_7 appeared as non-convex. This could be the result of premature convergence to a local minimum solution as opposed to the global optimum.
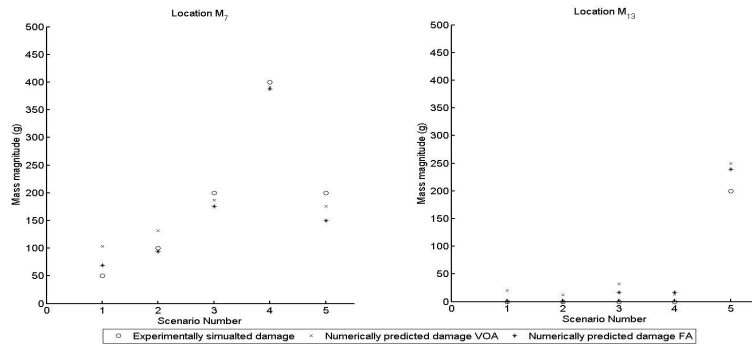

Figure 5 - Experimental masses and deterministic masses predicted by VOA and FA
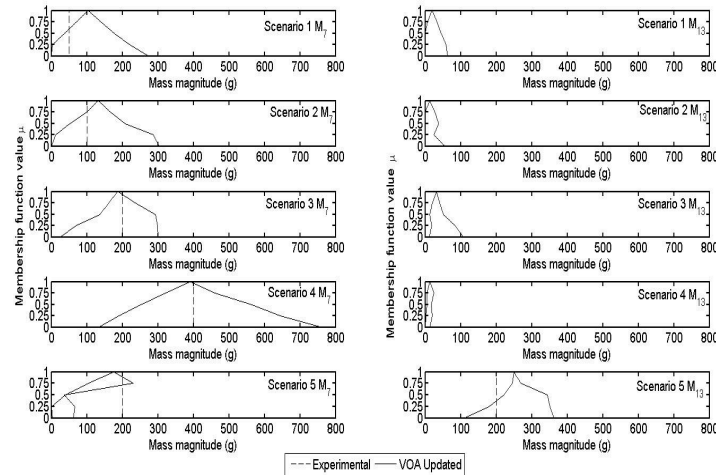

Figure 6 - Experimental masses and fuzzy masses obtained by VOA

4   Conclusions

Within this research, a SHM methodology was developed and implemented to facilitate damage severity assessment of a laboratory-scale wind turbine blade. The method demonstrated the ability to predict successfully the location and magnitude of structural alteration on the blade. Uncertainty due to measurement and modelling error was incorporated through modelling responses as fuzzy numbers with triangular membership functions to obtain the uncertainty associated with input parameters. VOA was proposed and undertaken for minimisation of the

objective functions using FFEMU and was found to be satisfactory for the purpose. To compare the accuracy of VOA, we judged the algorithm ability to reach the global minimum presumed to have been achieved by PSO and FA. Often, VOA was able to achieve an objective function value close to the other algorithms, but equally often displayed convergence on a higher value. In terms of computational efficiency, due to the dynamic nature of the algorithm population size, VOA was found to require significantly more function evaluations before convergence than either PSO or FA.

Acknowledgements

References

[1] Fischer, K., Besnard, F. and Bertling, L., (2012). Reliability-centered maintenance for wind turbines based on statistical analysis and practical experience, *IEEE Transactions on Energy Conversion,* **27**(1), pp. 184-195.

[2] Doebling, S., Farrar, C. and Prime, M., (1998). A summary review of vibration based damage identification methods, *The Shock and Vibration Digest,* pp. 91-105.

[3] Hua, X.G., Ni, Y.Q., Chen, Z.Q. and Ko, J.M., (2008). An improved perturbation method for stochastic finite element model updating, *International Journal for Numerical Methods in Engineering,* **73**(13), pp. 1845-1864.

[4] Behmanesh, I. and Moaveni, B., (2015). Probabilistic identification of simulated damage on the Dowling Hall Footbridge through Bayesian finite element model updating, *Structural Control and Health Monitoring,* **22**(3), pp. 463-483.

[5] Chandrashekhar, M. and Ganguli, R., (2009). Uncertainty handling in structural damage detection using fuzzy logic and probabilistic simulation, *Mechanical Systems and Signal Processing,* **23**(2), pp. 384-404.

[6] Simoen, E., de Roeck, G. and Lombaert, G., (2015). Dealing with uncertainty in model updating for damage assessment: A review, *Mechanical Systems and Signal Processing,* **56**, pp. 123-149.

[7] Erdogan, Y.S., Bakir, P.G., Gul, M. and Catbas, F.N., (2013). Investigation of the effect of model uncertainties on structural response using structural health monitoring data, *Journal of Structural Engineering, ASCE,* **140**(11)*,* pp. 2451-2457.

[8] Liu, Y. and Duan, Z., (2012). Fuzzy finite element model updating of bridges by considering the uncertainty of the measured modal parameters, *Science China Technological Sciences,* **55**(11), pp. 3109-3117.

[9] Khodaparast, H.H., Govers, Y., Dayyani, I., Adhikari, S., Link, M., Friswell, M.I., Mottershead, J.E. and Sienz, J., (2017). Fuzzy finite element model updating of the DLR AIRMOD test structure, *Applied Mathematical Modelling,* **52**(Supplement C), pp.512-526.

[10] Turnbull, H., and Omenzetter, P., (2018). Comparison of two optimization algorithms for fuzzy finite element model updating for damage detection in a wind turbine blade, *Proc. 2018 SPIE Smart Structures/Non-destructive Evaluation Conference*, pp. 105991Q-10599-14.

[11] Brincker, R. and Ventura, C.E., (2015). Frequency-domain identification, In *Introduction to Operational Modal Analysis,* Wiley, pp. 261-280.

[12] Soden, P.D., Hinton, M.J. and Kaddour, A.S., (1998). Lamina properties, lay-up configurations and loading conditions for a range of fibre-reinforced composite laminates, *Composites Science & Technology,* **58**(7), pp. 1011-1022.

[13] Zadeh, L.A., (1965). Fuzzy sets, *Information and Control,* **8**(3), pp. 338-353.

[14] Liang, Y. and Cuevas Juarez, J.R., (2016). A novel metaheuristic for continuous optimization problems: Virus optimization algorithm, *Engineering Optimization,* **48**(1), pp. 73-93.

[15] Ciang, C.C., Lee, J. and Bang, H., (2008). Structural health monitoring for a wind turbine system: A review of damage detection methods, *Measurement Science & Technology,* **19**(12), pp. 20.

[16] Ataya, S. and Ahmed, M.M.Z., (2013). Damages of wind turbine blade trailing edge: Forms, location, and root causes, *Engineering Failure Analysis,* **35,** pp. 480-488.

[17] Papazafeiropoulos, G., Muñiz-Calvente, M. and Martínez-Pañeda., E., (2017). Abaqus2Matlab: A suitable tool for finite element post-processing, *Advances in Engineering Software,* **105**, pp. 9-16.